© 2018. Published by The Company of Biologists Ltd | Development (2018) 145, dev170670. doi:10.1242/dev.170670

RESEARCH ARTICLE

The microRNAs let-7 and miR-278 regulate insect metamorphosis and oogenesis by targeting the juvenile hormone early-response gene *Krüppel-homolog 1*

Jiasheng Song, Wanwan Li, Haihong Zhao, Lulu Gao, Yuning Fan and Shutang Zhou*

ABSTRACT

Krüppel-homolog 1 (Kr-h1), a zinc-finger transcription factor, inhibits larval metamorphosis and promotes adult reproduction by transducing juvenile hormone (JH). Although the transcriptional regulation of *Kr-h1* has been extensively studied, little is known about its regulation at the post-transcriptional level. Using the migratory locust *Locusta migratoria* as a model system, we report here that the microRNAs let-7 and miR-278 bound to the *Kr-h1* coding sequence and downregulated its expression. Application of let-7 and miR-278 mimics (agomiRs) significantly reduced the level of *Kr-h1* transcripts, resulting in partially precocious metamorphosis in nymphs as well as markedly decreased yolk protein precursors, arrested ovarian development and blocked oocyte maturation in adults. Moreover, the expression of let-7 and miR-278 was repressed by JH, constituting a regulatory loop of JH signaling. This study thus reveals a previously unknown regulatory mechanism whereby JH suppresses the expression of let-7 and miR-278, which, together with JH induction of *Kr-h1* transcription, prevents the precocious metamorphosis of nymphs and stimulates the reproduction of adult females. These results advance our understanding of the coordination of JH and miRNA regulation in insect development.

KEY WORDS: MicroRNA, Kr-h1, Juvenile hormone, Metamorphosis, Female reproduction

INTRODUCTION

Insect development, metamorphosis and reproduction are primarily controlled by juvenile hormone (JH) and 20-hydroxyecdysone (20E). Whereas 20E initiates larval/nymphal molting and metamorphosis, JH maintains the juvenile status by repressing the metamorphic action of 20E (Jindra et al., 2015a, 2013; Riddiford, 1994). JH also stimulates aspects of female reproduction, including previtellogenic development, vitellogenesis and oogenesis, in many insect species (Raikhel et al., 2005; Roy et al., 2018; Wyatt and Davey, 1996). The molecular action of JH relies on its intracellular receptor Methoprene-tolerant (Met), a member of basic helix-loop-helix Per-Arnt-Sim (bHLH-PAS) transcription factor family (Charles et al., 2011; Jindra et al., 2015b; Li et al., 2011). JH induces the heterodimerization of Met with another bHLH-PAS protein, Taiman (Tai), to form an active JH-receptor complex that regulates the transcription of JH-responsive genes (Guo et al., 2014; Kayukawa et al., 2012; Li et al., 2011; Luo et al., 2017; Wu et al., 2018b). Krüppel-homolog 1 (Kr-h1), a C_2H_2 zinc-finger transcription factor, is a key player in JH signaling pathway. The JH-induced Met/Tai complex binds to the JH response element in the promoter of *Kr-h1* and directly activates its transcription (Cui et al., 2014; Kayukawa et al., 2012; Li et al., 2014; Lozano et al., 2014; Shin et al., 2012; Song et al., 2014). During the larval stage, Kr-h1 transduces the anti-metamorphic action of JH in both holometabolous and hemimetabolous insects (Konopova et al., 2011; Lozano and Belles, 2011; Minakuchi et al., 2009, 2008). Kr-h1 prevents immature larvae from initiating precocious larval-pupal transition by repressing the expression of the pupal specifier gene *Broad-complex* (*BR-C*) (Jindra et al., 2013). Kr-h1 also inhibits precocious adult metamorphosis by suppressing the expression of the adult specifier gene *Ecdysone induced protein 93F* (*E93*) (Belles and Santos, 2014). Recent studies have demonstrated that Kr-h1 binds to the consensus Kr-h1 binding site (KBS) in the promotor regions of *BR-C* and *E93* to directly suppress their transcription (Kayukawa et al., 2017, 2016). Moreover, Kr-h1 can function as an antagonist of 20E synthesis by directly inhibiting the transcription of genes coding for steroidogenic enzymes in prothoracic glands of the fruit fly *Drosophila melanogaster* and the silkworm *Bombyx mori* (Liu et al., 2018; Zhang et al., 2018). The role of Kr-h1 in JH-regulated female reproduction appears to vary among insect species. In the mosquito *Aedes aegypti*, Kr-h1 can activate and repress the expression of its target genes for previtellogenic development and egg production in response to JH (Ojani et al., 2018; Shin et al., 2012; Zou et al., 2013). Depletion of *Kr-h1* in adult females of the common bed bug *Cimex lectularius* does not reduce the egg number but severely reduces the egg hatchability (Gujar and Palli, 2016). In the migratory locust *Locusta migratoria*, Kr-h1 mediates JH action to promote vitellogenesis, ovarian development and oocyte maturation (Song et al., 2014). Although extensive studies have been conducted to elucidate the transcriptional activation of *Kr-h1* and its regulation of target genes, microRNA (miRNA)-mediated regulation of *Kr-h1* at the post-transcriptional level has been less explored.

miRNAs are ∼22-nucleotide non-coding RNAs, that bind complementarily to the 3′-untranslated region (3′UTR) or the coding sequence (CDS) of target mRNAs to regulate gene expression at the post-transcriptional level (Forman et al., 2008; Ghildiyal and Zamore, 2009; Rigoutsos, 2009). Previously, only miR-2 has been demonstrated to target *Kr-h1*. In the cockroach *Blattella germanica*, miR-2 eliminates *Kr-h1* transcripts at the final nymphal instar, which, together with the decrease of JH and concomitant reduction of *Kr-h1* transcription, ensures the onset of metamorphosis (Lozano et al., 2015). miRNAs can also interact with the 20E pathway to modulate insect metamorphosis and reproduction (Belles, 2017; Belles et al., 2012; Lucas and Raikhel,

Key Laboratory of Plant Stress Biology, State Key Laboratory of Cotton Biology, School of Life Sciences, Henan University, Kaifeng 475004, China.

*Author for correspondence (szhou@henu.edu.cn)

L.G., 0000-0003-1334-3742; S.Z., 0000-0003-4881-3644

Received 8 August 2018; Accepted 14 November 2018

Development (2018) 145, dev170670. doi:10.1242/dev.170670

2013; Roy et al., 2018). The let-7 cluster, which includes let-7, miR-100 and miR-125, is regulated by 20E, targeting the *abrupt* gene and controlling neuromuscular and wing development during the metamorphosis of *D. melanogaster* (Caygill and Johnston, 2008; Chawla and Sokol, 2012). In *B. mori*, let-7 exerts its function in larval-pupal transition by targeting the 20E response genes *FTZ-F1* and *E74* (Ling et al., 2014). In vitellogenic adult females of *Ae. aegypti*, 20E-dependent expression of miR-275 is required for blood digestion, and inhibition of miR-275 leads to incomplete egg development (Bryant et al., 2010). Mosquito-specific miR-1890 is also activated by the 20E pathway, which affects ovarian development by targeting the serine protease gene *JHA15* (Lucas et al., 2015). Despite the understanding of miRNA regulation in 20E-triggered insect metamorphosis and reproduction, little is known about the interaction of miRNAs with the JH signaling pathway in JH-stimulated vitellogenesis and oogenesis.

L. migratoria has been used widely as a model for studying the mechanisms of JH-dependent female reproduction, as JH controls Vitellogenin (Vg; the yolk protein precursor) synthesis in the fat body, secretion into the hemolymph and uptake by the maturing oocytes (Raikhel et al., 2005; Roy et al., 2018; Wyatt and Davey, 1996). In the present study, we performed high-throughput miRNA sequencing and quantification to identify miRNAs involved in the JH pathway. We found that let-7 and miR-278 were regulated by JH and targeted *Kr-h1* by binding to its CDS. The expression of let-7 and miR-8 increased at the final nymphal instar, but decreased in both previtellogenic and vitellogenic stages. Injection of let-7 and miR-278 agomiRs led to markedly reduced Vg protein, blocked oocyte maturation and impaired ovarian growth in adult female locusts as well as moderate phenotypes of precocious metamorphosis in nymphs. This study thus points to a previously unidentified mechanism by which JH-suppressed miRNAs regulate insect metamorphosis and reproduction by targeting an early JH-response gene.

RESULTS

Identification of miRNAs targeting *Kr-h1*

L. migratoria has abundant miRNAs in its genome (Wang et al., 2015). To elucidate the regulatory mechanisms of miRNA in JH-stimulated vitellogenesis and egg production, we performed high-throughput sequencing with small RNA libraries derived from the fat body of adult female locusts within 12 h of post-adult emergence (0 day PAE) as well as those at 2, 4 and 6 days PAE. In total, 483 miRNAs were identified and 335 miRNAs were found with RPKM values >10. Of these candidate miRNAs, we chose to focus on the conserved miRNAs because of their crucial role in insect development and conservation across insect orders. Of those with RPKM values >10, a total of 60 conserved miRNAs were identified by similarity search against miRBase database (Fig. S1A) (Kozomara and Griffiths-Jones, 2014). These conserved miRNAs could be categorized into five hierarchical clusters by complete linkage algorithm with the respective read counts (Fig. 1A). Group 1, consisting of ten miRNAs, showed a general increase of expression from 0 to 6 days PAE. The levels of six miRNAs (Group 2) were increased at 2-4 days PAE and then declined at 6 days PAE. In Group 3, comprising 17 miRNAs, most were expressed at gradually lower levels from 2 to 6 days PAE. The expression of ten miRNAs (Group 4) was decreased at 2 days PAE but thereafter elevated at 4-6 days PAE. The levels of 16 miRNAs (Group 5) were lower at 2-4 days PAE and continued to drop on day 6. Based on the cutoff criteria at fold change >1.5 and $P<0.05$, the levels of 24, 22 and 25 miRNAs were significantly declined at 2, 4 and 6 days PAE, respectively, compared with day 0 (Fig. S1B). In the first gonadotrophic cycle, adult female locusts underwent previtellogenesis from 0 to 4 days PAE and vitellogenesis started at ∼5 days PAE under our rearing conditions. The above data indicate that most of conserved miRNAs identified from our large-scale small RNA sequencing are expressed at lower levels during the previtellogenic development and vitellogenesis, compared with that on the day of adult ecdysis.

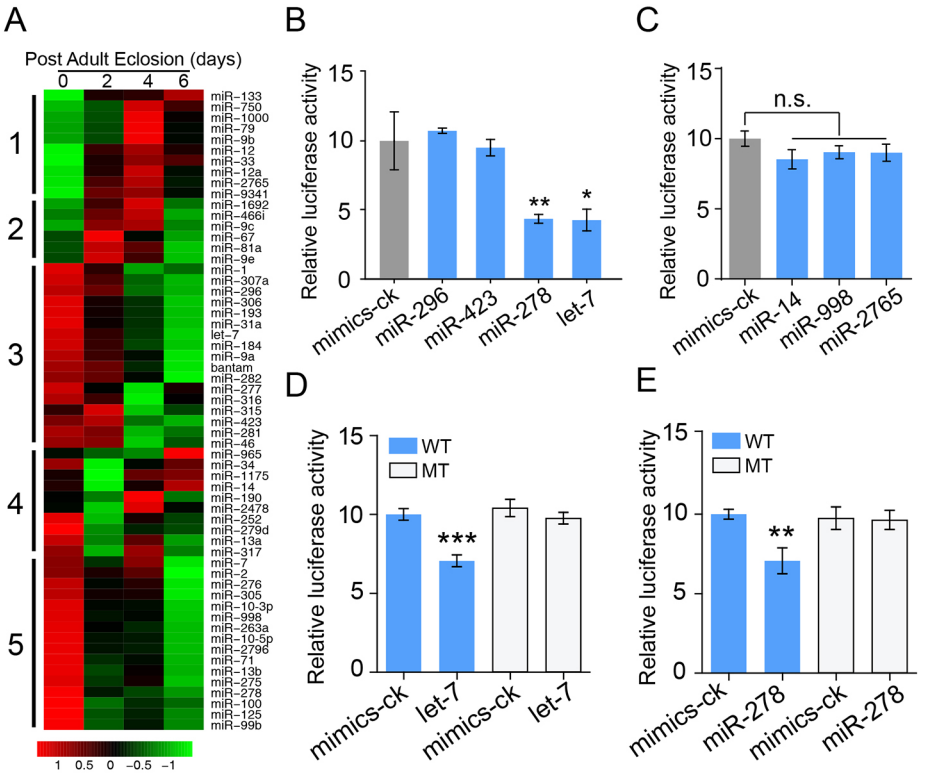

Fig. 1. Identification of miRNAs potentially targeting *Kr-h1*. (A) Heatmap indicating the temporal expression patterns of 60 conserved miRNAs identified from small RNA sequencing and quantification of fat bodies collected from adult female locusts at 0, 2, 4 and 6 days post-adult eclosion. Numbers on the left indicate the classified groups of miRNAs. Numbers below the bar indicate normalized log10 values of read counts. (B) Dual-luciferase reporter assays using HEK293T cells co-transfected with miRNA mimics and recombinant pmirGLO vectors containing the predicted binding sites of miR-296, miR-423, let-7 and miR-278 in the CDS of *Kr-h1*. *$P<0.05$, **$P<0.01$, compared with the negative control of mimics (mimics-ck). $n=6$. (C) Dual-luciferase reporter assays using HEK293T cells co-transfected with miRNA mimics and recombinant pmirGLO vectors containing the predicted binding sites of miR-14, miR-998 and miR-2765 in the 3′UTR of *Kr-h1*. n.s., no significant difference. $n=6$. (D,E) Dual-luciferase reporter assays using HEK293T cells co-transfected with let-7 mimics (D) or miR-278 mimics (E) plus recombinant pmirGLO vectors containing either wild-type (WT) or mutated (MT) binding sites of let-7 or miR-278. **$P<0.01$, ***$P<0.001$, compared with the negative control of mimics (mimics-ck). $n=6$.

Development (2018) 145, dev170670. doi:10.1242/dev.170670

We next predicted the miRNA-binding sites of *Kr-h1* (GenBank: KJ425482) mRNA to identify the conserved miRNAs potentially involved in *Kr-h1* regulation. Seven conserved miRNAs were predicted to bind to *Kr-h1* mRNA sequence. The binding sites of let-7, miR-278, miR-423 and miR-296 were in the CDS (Fig. S1C), whereas miR-14, miR-998 and miR-2765 presumably bound to the 3′UTR (Fig. S1D). To validate the binding of predicted miRNAs to *Kr-h1* mRNA, we carried out dual-luciferase reporter assays by co-transfection of miRNA mimics and a recombinant pmirGLO vector with ∼500-bp DNA fragments containing the predicted miRNA-binding sites into HEK293T cells. When let-7 and miR-278 mimics were transfected, luciferase activities declined by 57% and 56%, respectively, compared with the non-mimic controls (Fig. 1B). However, transfection with miR-296, miR-423, miR-14, miR-998 or miR-2765 mimics had no significant effect on the reporter activity (Fig. 1B,C). Knowing that let-7 and miR-278 suppressed the *Kr-h1* reporter activity, we mutated the binding sites complementary to the 'seed' sequences of let-7 or miR-278 (Fig. S1C) for further dual-luciferase assays. As shown in Fig. 1D,E, the capacity of let-7 or miR-278 to inhibit the *Kr-h1* reporter activity was completely blocked when the mutated sequences were employed. These observations suggest that let-7 and miR-278 bind to the CDS of *Kr-h1* to regulate its expression.

let-7 and miR-278 regulate *Kr-h1* expression *in vivo*

To reveal the dynamics of let-7 and miR-278 expression in the first gonadotrophic cycle, qRT-PCR was conducted using small RNAs isolated from the fat body of adult females at 0-8 days PAE. Compared with that at 0 day PAE, the expression levels of let-7 were significantly decreased by ∼67% on days 2-8 (Fig. 2A); miR-278 expression was significantly declined by 63-68% on days 2-4 and further decreased by 77-79% at 6-8 days PAE (Fig. 2B). A fall in the transcript levels of let-7 and miR-278 appeared to occur concurrently with elevated mRNA levels of *Kr-h1* (Fig. 2A,B) (Song et al., 2014). To evaluate the responsiveness of let-7 and miR-278 to JH, qRT-PCR was performed using small RNAs extracted from the fat body of JH-deprived adult females by ablation of the corpora allata with ethoxyprecocene treatment for 10 days (Dhadialla et al., 1987; Zhou et al., 2002) as well as those further treated with a potent JH analog, methoprene, for 6-48 h. As shown in Fig. 2C,E, chemical allatectomy by ethoxyprecocene treatment resulted in 1.4-fold and 1.5-fold increase of let-7 and miR-278 expression levels, respectively. Further application of methoprene led to 36% reduction of let-7 expression levels at 48 h (Fig. 2D). The levels of miR-278 declined by 31% and 51%, respectively, after methoprene treatment for 24 h and 48 h (Fig. 2F). As the miRNA-Ago1 complex is the key component of the RNA-induced silence complex (RISC), which is responsible for post-transcriptional regulation of target genes, we performed RNA immunoprecipitation (RIP) in the fat body using a monoclonal antibody against locust Argonaute 1 (Ago1) (Yang et al., 2014) to determine the interaction of let-7 and miR-278 with *Kr-h1* mRNA *in vivo*. agomiRs, chemically modified miRNA mimics, are widely used for miRNA function study *in vivo*, as they have the same effect as overexpression of the same miRNA. Injection of agomiR elevates the total abundance of this miRNA, though it does not cause the overexpression of endogenous miRNA. When let-7 agomiR was injected, the abundance of precipitated *Kr-h1* mRNA was 4.2-fold higher than the negative control (Fig. 3A). Injection of miR-278 agomiR led to a 3.3-fold increase of precipitated *Kr-h1* mRNA relative to the negative control (Fig. 3A). These data indicate *in vivo* binding of let-7 and miR-278 to *Kr-h1* mRNA.

We next evaluated the effect of let-7 and miR-278 agomiR treatment on *Kr-h1* transcript and protein levels. qRT-PCR demonstrated that *Kr-h1* transcripts reduced by 61% and 43% in the fat body of adult females injected with let-7 and miR-278 agomiRs, respectively (Fig. 3B). Western blot and subsequent quantification of band intensity showed that Kr-h1 protein levels declined to 65% and 47%, respectively of its normal levels after let-7 and miR-278 agomiR treatment (Fig. 3C,D). Taken together, the above results indicate that *Kr-h1* is downregulated by let-7 and miR-278.

Injection of let-7 and miR-278 agomiRs blocks vitellogenesis and egg production

Because let-7 and miR-278 were found to target *Kr-h1* and were expressed at low levels in the vitellogenic phase, we investigated their function in locust vitellogenesis and egg production by agomiR treatment. All phenotypes were examined at 8 days PAE,

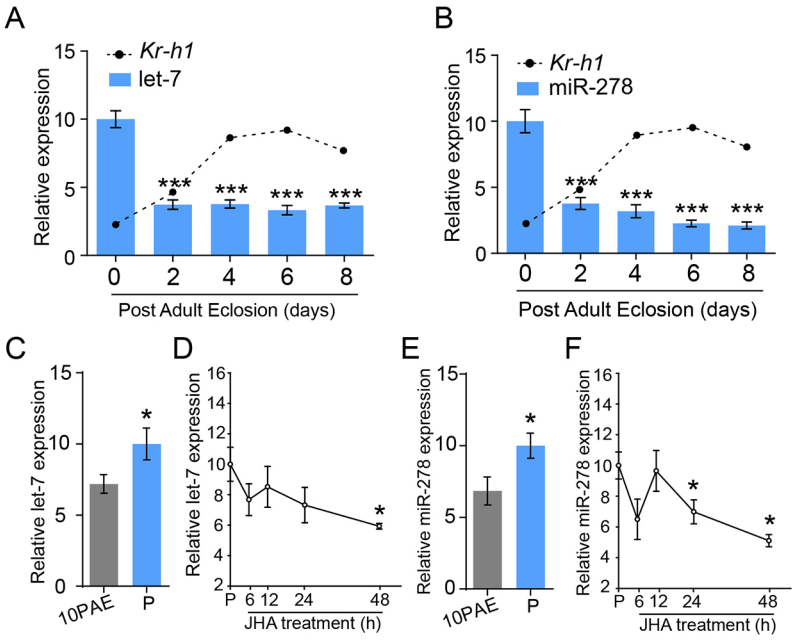

Fig. 2. Temporal expression patterns of let-7 and miR-278 and their responsiveness to JH. (A,B) Developmental profiles of let-7 (A) and miR-278 (B) in the fat body of adult females collected at 0, 2, 4, 6 and 8 days post-adult eclosion. The dashed lines indicate the expression pattern of *Kr-h1*, as a parallel comparison. ***P<0.001, compared with that on the day of adult eclosion (day 0). n=8. (C-F) The relative levels of let-7 (C,D) and miR-278 (E,F) expression in the fat body of adult females collected at 10 days post-adult eclosion (10PAE) as well as those treated with ethoxyprecocene (P) for 10 days and further treated with methoprene (JHA) for 6-48 h. *P<0.05, compared with 10PAE (C,E) (n=14) or compared with P (D,F) (n=8).

Development (2018) 145, dev170670. doi:10.1242/dev.170670

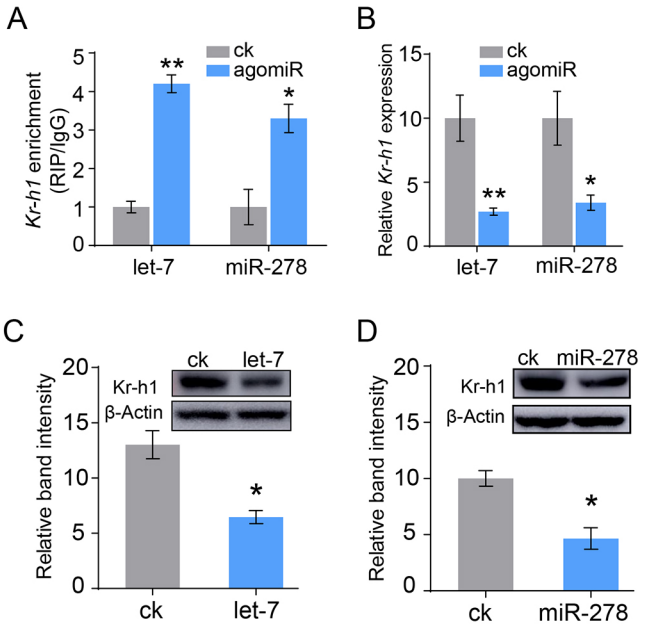

Fig. 3. let-7 and miR-278 bind *Kr-h1* mRNA and downregulate its expression *in vivo*. (A) RNA immunoprecipitation (RIP) showing the relative abundance of precipitated *Kr-h1* mRNA in the fat body of adult females injected with let-7 and miR-278 agomiRs. **P*<0.05, ***P*<0.01, compared with the negative controls (ck). *n*=4. (B) qRT-PCR showing the effect of let-7 and miR-278 agomiR treatment on *Kr-h1* mRNA levels in the fat body of adult females. **P*<0.05, ***P*<0.01, compared with the negative controls (ck). *n*=10. (C,D) Western blots and subsequent quantification of band intensity showing the effect of let-7 (C) and miR-278 (D) agomiR treatment on Kr-h1 protein levels in the fat body of adult females. **P*<0.05, compared with the negative controls (ck). *n*=3.

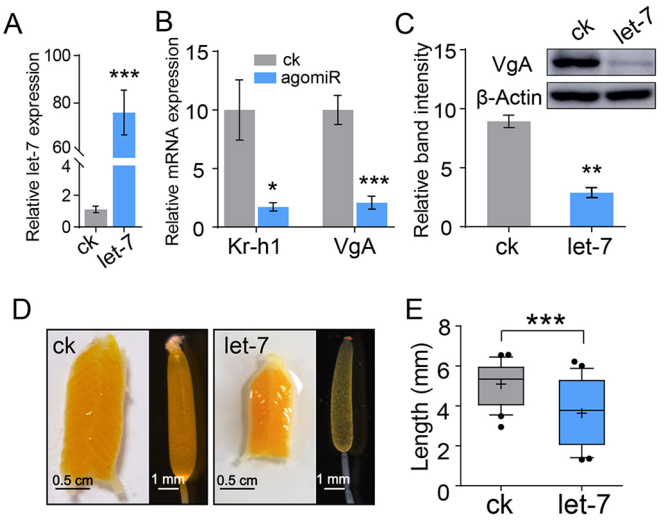

Fig. 4. Effect of let-7 agomiR treatment on locust vitellogenesis, oocyte maturation and ovarian growth. (A) Relative abundance of let-7 in the fat body of adult females injected with let-7 agomiR versus the negative control (ck). ****P*<0.001, compared with the negative control (ck). *n*=10-12. (B) Relative levels of *Kr-h1* and *VgA* mRNAs in the fat body of adult females injected with let-7 agomiR versus the negative control (ck). **P*<0.05, ****P*<0.001. *n*=12. (C) Western blot and quantification of band intensity showing the decrease of VgA protein levels after let-7 agomiR treatment. ***P*<0.01, compared with the negative control (ck). *n*=3. (D) Representative phenotypes of ovaries and primary oocytes after let-7 agomiR treatment versus the negative control (ck). (E) Comparison of primary oocyte lengths in the let-7 agomiR treatment group and the negative control group (ck). The box shows the minimum, median and maximum values and the whiskers represent the 10th and 90th percentiles. ****P*<0.001. *n*=12.

when *Vg* expression naturally reaches its peak and the primary oocytes are maturing. Compared with that of the negative controls, the total abundance of let-7 (which represents both endogenous let-7 and injected agomiR) was elevated by 76-fold in the fat body of adult females injected with let-7 agomiR (Fig. 4A). After let-7 agomiR treatment, the transcript levels of *Kr-h1* reduced by 73% (Fig. 4B). In *L. migratoria*, two *Vg* genes, *VgA* (GenBank: KF171066) and *VgB* (GenBank: KX709496), are coordinately expressed in a similar pattern (Dhadialla et al., 1987). *VgA* was selected as a representative. In let-7 agomiR-treated fat bodies, *VgA* mRNA levels decreased by 79% (Fig. 4B). Western blot and band intensity quantification demonstrated that injection of let-7 agomiR caused a 71% reduction of VgA protein levels in the fat body (Fig. 4C). Application of let-7 agomiR resulted in blocked maturation of primary oocytes and arrested growth of ovaries. Consequently, the primary oocytes and ovaries of let-7 agomiR-treated adult females were markedly smaller than that of the negative controls (Fig. 4D). Statistically, the average length of primary oocytes of let-7 agomiR-treated locusts was 3.7 mm, significantly smaller than that of negative controls (5.1 mm) (Fig. 4E).

As for miR-278, its total abundance increased by 38-fold after injection of miR-278 agomiR (Fig. 5A). The levels of *Kr-h1* transcript dropped by 57% in miR-278 agomiR-treated fat bodies compared with that in the negative controls. As a result, *VgA* mRNA and protein reduced to 25% and 53%, respectively, of their normal levels in the fat body (Fig. 5B,C). miR-278 agomiR-treated locusts also showed impaired oocyte maturation and ovarian growth (Fig. 5D), with significantly smaller primary oocytes (3.5 mm) in comparison with the negative controls (5.1 mm) (Fig. 5E). The defective phenotypes of ovarian growth and oocyte maturation caused by let-7 and miR-278 agomiR treatment resembled that resulting from *Kr-h1* RNAi, though at less severe levels (Song et al., 2014). Collectively, the above observations indicate a pivotal role of let-7 and miR-278 in locust female reproduction.

Application of let-7 and miR-278 agomiRs causes partially precocious metamorphosis

Kr-h1 has a dual role in preventing juvenile metamorphosis and promoting adult reproduction. We next investigated the involvement of let-7 and miR-278 in locust metamorphosis. Compared with the early penultimate 4th instar (N4), let-7 expression significantly increased by 2.2-fold in the whole body of middle 5th instar nymph (N5), and slightly declined to 2.0-fold at late N5, although this decline was not statistically significant (Fig. S2A). The expression levels of miR-278 were significantly elevated by 2.4-fold at early N5, then dropped at middle N5, but increased again by 1.7-fold (compared with that at middle N5) at late N5 (Fig. S2B). The elevated expression levels of let-7 and miR-278 at the final nymphal instar appeared to oppose the decreased levels of *Kr-h1* transcript at this stage (Fig. S2C). To explore the role of let-7 and miR-278 in locust metamorphosis, we treated penultimate 4th instar nymphs with let-7 and miR-278 agomiRs and examined the resulting phenotypes at 5th instar. After their respective agomiR treatment, the total abundance of let-7 and miR-278 increased by 16.2-fold and 10.1-fold, respectively, compared with the negative controls (Fig. 6A,B). Injection of let-7 and miR-278 agomiRs reduced *Kr-h1* transcripts by 54% and 48%, respectively, in the whole body at N5 (Fig. 6C). After let-7 agomiR treatment, 25% of N5 nymphs (three replicates with 16 locusts in each treatment) showed precocious adult-specific color

Development (2018) 145, dev170670. doi:10.1242/dev.170670

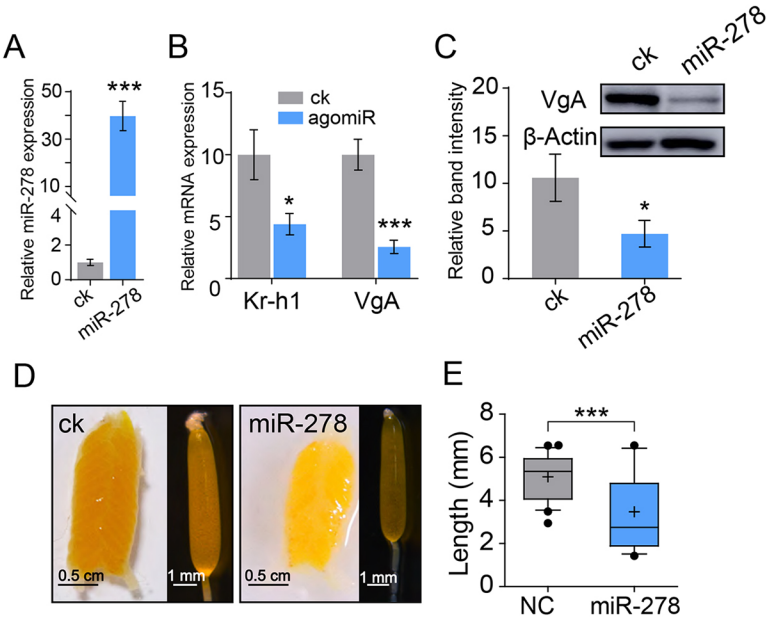

Fig. 5. Effect of miR-278 agomiR treatment on locust vitellogenesis, oocyte maturation and ovarian growth. (A) Relative abundance of miR-278 in the fat body of adult females injected with miR-278 agomiR versus the negative control (ck). ***P<0.001. n=12. (B) Relative levels of *Kr-h1* and *VgA* mRNAs in the fat body of adult females injected with miR-278 agomiR versus the negative control (ck). *P<0.05, ***P<0.001. n=12. (C) Western blot and quantification of band intensity showing the decrease of VgA protein levels after miR-278 agomiR treatment. *P<0.05, compared with the negative control (ck). n=3. (D) Representative phenotypes of ovaries and primary oocytes after miR-278 agomiR treatment vs the negative control (ck). (E) Comparison of primary oocyte lengths in the miR-278 agomiR treatment group and the negative control group (ck). The box shows the minimum, median and maximum values and the whiskers represent the 10th and 90th percentiles. ***P<0.001. n=12.

patterns in the pronotum, and 25% of N5 nymphs had intermediate phenotypes (Fig. 6D). Similar phenotypes of precocious nymphal-adult transition have been previously reported for the hemimetabolous linden bug *Pyrrhocoris apterus* (Smykal et al., 2014). When miR-278 agomiR was applied, 12.5% of N5 nymphs (three replicates with 16 locusts in each treatment) showed adult-specific color patterns in the pronotum, whereas 37.5% of N5 nymphs had the intermediate phenotypes (Fig. 6D). Notably, the phenotypes of precocious metamorphosis resulting from let-7 and miR-278 agomiR treatment were less severe than that of *Kr-h1* knockdown (Fig. S3). Collectively, these observations suggest that let-7 and miR-278 have a modest regulatory role in locust metamorphosis.

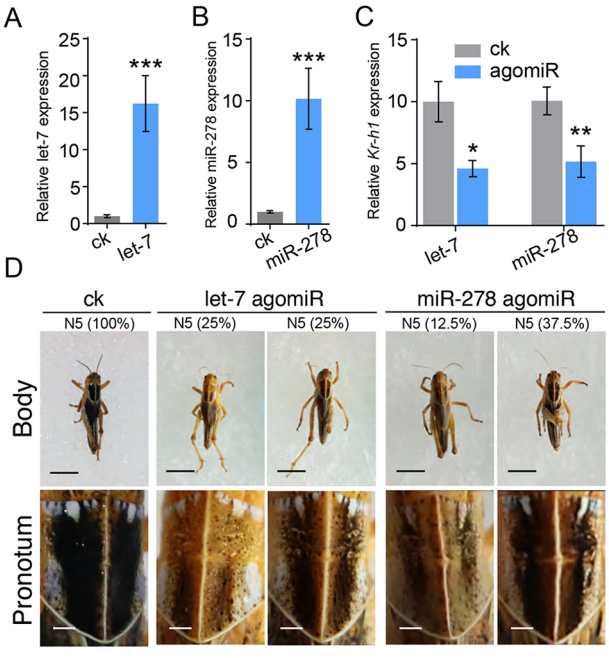

Fig. 6. Effect of let-7 and miR-278 agomiR treatment on locust metamorphosis. (A,B) The total abundance of let-7 (A) and miR-278 (B) in the whole body of final 5th instar nymphs previously subjected to the respective agomiR treatment at the penultimate 4th nymphal instar. ***P<0.001, compared with the negative controls (ck). n=16. (C) Effect of let-7 and miR-278 agomiR treatment on *Kr-h1* expression in the nymphs. agomiRs were injected at the penultimate 4th nymphal instar, and *Kr-h1* mRNA levels were measured in the whole body at the final 5th nymphal instar. *P<0.05, **P<0.01, compared with the negative controls (ck). n=26. (D) The representative phenotypes and percentage of partially precocious metamorphosis at the final 5th nymphal instar (N5), previously treated with let-7 and miR-278 agomiRs at the penultimate 4th nymphal instar (3 replicates with 16 locusts in each treatment). Upper panel, whole body. Lower panel, enlarged images of the pronotum. ck, the negative control. Scale bars: 1 cm (upper panels); 0.1 cm (lower panels).

DISCUSSION

Regulation of *Kr-h1* by let-7 and miR-278

As an early JH-response gene immediately downstream of the JH receptor, *Kr-h1* plays an indispensable role in insect metamorphosis and reproduction (Belles and Santos, 2014; Lozano and Belles, 2011; Ojani et al., 2018; Song et al., 2014; Ureña et al., 2016). The intracellular JH receptor complex binds to the JH response elements (E-box or E-box-like motif) in the promoter of *Kr-h1* and directly regulates its transcription (Cui et al., 2014; Kayukawa et al., 2012; Li et al., 2011; Shin et al., 2012; Song et al., 2014). In addition, *Kr-h1* is found to be post-transcriptionally regulated by miR-2 via binding to the 3′UTR of *Kr-h1* (Lozano et al., 2015). In the final instar nymphs of *B. germanica*, miR-2 scavenges *Kr-h1* transcripts, crucially contributing to the onset of metamorphosis (Lozano et al., 2015). In the present study, we performed high-throughput miRNA sequencing to identify miRNAs potentially regulating *Kr-h1*. Of seven conserved miRNAs with the predicted binding sites of *Kr-h1* mRNA, let-7 and miR-278 were documented to downregulate *Kr-h1* expression via binding to its CDS. Thus, our data extend the view of *Kr-h1* regulation at the post-transcriptional level. Interestingly, the miR-2 binding site was not predicted in the locust *Kr-h1* mRNA sequence by using the algorithms of miRanda, PITA and MicroTar, suggesting diversity of miRNA and target gene interaction in various insect species. Nevertheless, we cannot exclude the possible prediction of miR-2-binding sites of *Kr-h1* mRNA by using other predicting algorithms. It should be noted that TRIzol reagent was used for miRNA extraction in this study. It has been reported that miRNAs with low GC content might be lost during extraction with TRIzol (Kim et al., 2012).

Development (2018) 145, dev170670. doi:10.1242/dev.170670

A single miRNA usually has multiple targets, and multiple miRNAs can regulate a single gene (Bonci et al., 2008; Hashimoto et al., 2013). It has been demonstrated that let-7 regulates *abrupt*, *FTZ-F1* and *E74* to modulate molting and metamorphosis in *D. melanogaster* and *B. mori* (Caygill and Johnston, 2008; Ling et al., 2014). miR-278 targets *expanded*, *pyrethroid resistance-related gene* (*CYP6AG11*), and *insulin-related peptide binding protein 2* (*IBP2*) to modulate energy homeostasis, insecticide resistance and immune response in *D. melanogaster*, *B. mori* and the mosquito *Culex pipiens pallens* (Lei et al., 2015; Teleman et al., 2006; Wu et al., 2016). Intriguingly, the expression of let-7 and miR-278 was repressed by JH. Our results suggest that as well as acting through Met/Tai to induce *Kr-h1* transcription, JH also suppresses the expression of let-7 and miR-278 to maintain a proper level of Kr-h1, which is essential for suppressing precocious nymphal metamorphosis and promoting JH-dependent female reproduction in *L. migratoria*. In hemimetabolous *B. germanica*, JH represses the expression of let-7 that contributes to the formation of wings during metamorphosis, possibly through modulation of *BR-C* (Rubio and Belles, 2013; Rubio et al., 2012). In *D. melanogaster*, miR-14 targets *EcR*, whereas 20E represses the expression of miR-14, consequently leading to elevated EcR levels and amplified 20E signaling (Varghese and Cohen, 2007). A similar regulatory loop has also been reported for miR-281, EcR-B and 20E in *B. mori* (Jiang et al., 2013). These regulatory loops may typically represent the adaption of JH- and 20E-modulated gene regulation during the evolution of insect metamorphosis and reproduction.

let-7 and miR-278 in Kr-h1-mediated insect reproduction and metamorphosis

In a previous report, we have demonstrated that *Kr-h1* knockdown in adult female locusts causes substantial reduction of *Vg* expression as well as blocked oocyte maturation and arrested ovarian growth (Song et al., 2014). In this study, let-7 and miR-278 agomiR treatment caused significant reduction of *Kr-h1* transcripts. Application of let-7 and miR-278 agomiRs also markedly reduced the levels of *Vg* expression, accompanied by inhibited oocyte maturation and impaired ovarian growth. These observations provide evidence that let-7 and miR-278 are crucial players in JH-dependent locust vitellogenesis and egg production.

We also examined the effect of let-7 and miR-278 agomiR treatment on locust molting, as their target gene, *Kr-h1*, plays an essential role in repressing larval-pupal and larval-adult transition (Belles and Santos, 2014; Konopova et al., 2011; Lozano and Belles, 2011; Minakuchi et al., 2009, 2008). Application of let-7 and miR-278 agomiRs in penultimate instar nymphs caused partially precocious metamorphosis as shown by the presence of adult-specific patterns on the pronotum. Notably, the defective phenotypes of female reproduction and precocious metamorphosis caused by treatment of let-7 or miR-278 agomiRs were less severe than that resulting from *Kr-h1* RNAi, suggesting fine-tuning by miRNAs. Another possibility might be that some phenotypes are counteracted by other genes targeted by let-7 or miR-278. Moreover, *Kr-h1* transcript levels declined by 48-60% after let-7 and miR-278 agomiR treatment, whereas up to 92% knockdown efficiency was obtained with *Kr-h1* RNAi. The presence of more *Kr-h1* transcripts in agomiR-treated locusts than *Kr-h1*-depleted individuals might also attribute to these less severe phenotypes.

Based on our findings, we propose that as well as acting through its intracellular receptor to induce *Kr-h1* transcription, JH also represses the expression of let-7 and miR-278 to maintain the proper levels of Kr-h1 essential for metamorphosis and reproduction in locusts. At the final nymphal instar, the decreased JH titer and increased abundance of let-7 and miR-278 led to low levels of *Kr-h1* expression, contributing to the onset of metamorphosis. In previtellogenic and vitellogenic adult females, the increased JH titer and declined abundance of let-7 and miR-278 ensure high levels of *Kr-h1* expression, consequently stimulating the vitellogenesis and oogenesis.

MATERIALS AND METHODS

Ethics statement

Maintenance of and experiments on rabbits were approved by the Medical and Scientific Research Ethics Committee of Henan University.

Experimental animals

Gregarious-phase migratory locusts were reared under a 14h light:10 h dark photoperiod and at 30±2°C. The diet included a continuous supply of dry wheat bran with fresh wheat seedlings provided twice per day. JH-deprived adult female locusts were obtained by topical application of 500 µg (100 µg/µl dissolved in acetone) ethoxyprecocene (Sigma-Aldrich) per locust to inactivate the corpora allata within 12 h after adult emergence (Dhadialla et al., 1987; Zhou et al., 2002). To restore JH activity, s-(+)-methoprene (Santa Cruz Biotechnology) was topically applied at 150 µg (30 µg/µl dissolved in acetone) per locust 10 days post-ethoxyprecocene treatment as previously described (Dhadialla et al., 1987; Zhou et al., 2002).

Small RNA sequencing and data processing

Small RNA sequencing and quantification were performed with small RNA libraries derived from the fat body of adult females at 0, 2, 4 and 6 days post-adult emergence, using the Illumina HiSeq 2500 platform. The clean reads were obtained by eliminating low-quality reads, empty adapters, reads shorter than 18 nt, and reads with poly(A) tail. Sequences of tRNA, rRNA, snRNA, snoRNA and piRNA were removed by similarity search using the Rfam12.1 and piRNABank database. miRNAs were identified by blasting the rest sequences with miRBase (V21) and referring to the locust genome (Wang et al., 2014). miRanda (V3.3a) (Enright et al., 2003), PITA (V6) and MicroTar (V0.9.6) (Thadani and Tammi, 2006) were employed for prediction of miRNA-binding sites.

RNA extraction and qRT-PCR

Total RNA from the whole body and selected tissues was isolated using TRIzol reagent (Thermo Fisher), and cDNA was reverse transcribed with the FastQuant RT Kit (Tiangen). qRT-PCR was performed using a LightCycler 96 System (Roche) and the SuperReal PreMix Plus kit (Tiangen), initiated at 95°C for 2 min, followed by 40 cycles of 95°C for 20 s, 58°C for 20 s and 68°C for 20 s. For miRNA, cDNA was synthesized from total RNA using an miRNA first-strand cDNA synthesis kit (Tiangen). qRT-PCR for miRNA was conducted using Roche LightCycler system and miRcute miRNA qPCR kit (Tiangen) at 94°C for 2 min plus 40 cycles of 94°C for 20 s and 60°C for 34 s. Relative expression levels were calculated using the $2^{-\Delta\Delta Ct}$ method, with β-actin and U6 as the internal controls of gene and miRNA, respectively. Primers used for qRT-PCR are listed in Table S1.

Luciferase reporter assay

Kr-h1 cDNA fragments with miRNA-binding sites were cloned into pmirGLO vector (Promega) and confirmed by sequencing. For site mutation, the seed regions of let-7- and miR-278-binding sites were mutated to their complementary sequences using site-directed and ligase-independent mutagenesis (Chiu et al., 2004). The constructed vectors, miRNA mimics or the negative control (GenePharma) were then transfected into HEK293T cells (cells were kindly provided by Stem Cell Bank, Chinese Academy of Sciences) using Lipofectamine 3000 (Thermo Fisher). After 36 h, the luciferase activity was measured using the Dual-Glo Luciferase Assay System (Promega) and analyzed with GloMax 96 Microplate Luminometer (Promega). Primers used for site mutation are listed in Table S1.

RNA immunoprecipitation (RIP)

RIP experiments were performed using Magna RIP Kit (Millipore) according to the manufacturer's instructions. Briefly, freshly dissected fat

bodies were homogenized in ice-cold RIP lysis buffer, centrifuged for 15 min at 14,000 ***g***, and stored at −80°C overnight. After further centrifugation for 15 min at 14,000 ***g***, the supernatant was incubated at 4°C for 4 h with magnetic beads pre-incubated with a monoclonal antibody against locust Ago1 (Yang et al., 2014) or normal mouse IgG. The precipitated RNA was eluted and reverse transcribed to cDNA using Superscript IV reverse transcriptase and random hexamers (Thermo Fisher), followed by quantification using qRT-PCR.

RNA interference and agomiR treatment

For RNAi experiments, Kr-h1 and green fluorescent protein (GFP) dsRNAs were synthesized using T7 RiboMAX Express RNAi system (Promega). The 4th instar nymphs and adult females were intra-abdominally injected with 5 µg dsRNA within 24 h of nymphal molting and within 12 h of adult emergence, respectively. For agomiR treatment, 4th instar nymphs within 24 h of molting and adult females within 12 h of adult emergence were intra-abdominally injected with 0.5 nmol and 1 nmol agomiR (GenePharma), respectively, mixed with *in vivo* RNA Transfection Reagent (Engreen). A sequence from *Caenorhabditis elegans* genome (sense: 5′-UUCUCCGAACGUGUCACG-UTT-3′; antisense: 5′-ACGUGACACGUUCGGAGAATT-3′) was used as the negative control of agomiR (Sun et al., 2013; Wu et al., 2018a). Treatment of agomiR on adult females was repeated (using the same amount and concentration) twice, on day 3 and day 6.

Kr-h1 antibody preparation

A 756-bp cDNA fragment coding for a 252-aa peptide (forward primer: 5′-CGGGGTACCTACAAGTGCGACGTGTGCGA-3′; reverse primer: 5′-CCGGAATTCCAGGTAGTAGTAGCAGAGGT-3′) of locust *Kr-h1* was cloned into pET-32a-His and confirmed by sequencing. The recombinant Kr-h1 peptide was purified using an NTA-Ni2+-affinity column (CWBIO) and examined by SDS-PAGE. Polyclonal antibody against Kr-h1 was raised in rabbits using the Kr-h1 peptide mixed with Freund's complete adjuvant (Sigma-Aldrich) to form a stable emulsion for immunization. The New Zealand White rabbits (*Oryctolagus cuniculus*) were injected subcutaneously at four sites and boosted once a week for a total of four times. The antiserum specificity was verified by western blot using protein extracts from the fat body treated with dsKr-h1 vs dsGFP (Fig. S4).

Western blot

Total proteins were extracted from the whole body of nymphs or the fat body of adult females using lysis buffer containing 50 mM Tris-HCl (pH 7.5), 150 mM NaCl, 2 mM EDTA, 1 mM DTT, 1% Triton X-100, 1 mM PMSF and a protease inhibitor cocktail (Roche). The tissue lysates were then cleared by centrifugation at 12,000 ***g*** at 4°C for 30 min. Extracted proteins were quantified using a BCA protein assay kit (Pierce), fractionated on 8% SDS-PAGE, and then transferred to PVDF membranes (Millipore). Western blot was carried out using antibodies against locust Kr-h1 (1:2000) and VgA (1:5000) (Luo et al., 2017). β-actin (BM5422, BOSTER, 1:10,000) was used as a loading control. The corresponding HRP-conjugated secondary antibody (goat anti-rabbit IgG, BA1054, BOSTER, 1:10,000) and enhanced ECL Western Blotting Substrate (BOSTER) were employed for chemiluminescence. Bands were imaged with an Amersham Imager 600 (GE Healthcare) and analyzed using ImageJ software.

Data analysis

Statistical analyses were performed by Student's *t*-test or one-way ANOVA with LSD (least significant difference) post-hoc tests using SPSS 21.0 software. Values are shown as mean±s.e.m. and significant difference was considered at $P<0.05$.

Acknowledgements

Competing interests

The authors declare no competing or financial interests.

Author contributions

Conceptualization: J.S., S.Z.; Methodology: J.S., W.L., H.Z., S.Z.; Software: J.S., S.Z.; Validation: J.S., W.L., H.Z., L.G., Y.F., S.Z.; Formal analysis: J.S., S.Z.; Investigation: J.S., W.L., H.Z., L.G., Y.F., S.Z.; Resources: J.S., S.Z.; Data curation: J.S., W.L., H.Z., S.Z.; Writing - original draft: J.S., S.Z.; Writing - review & editing: J.S., S.Z.; Visualization: J.S., S.Z.; Supervision: J.S., S.Z.; Project administration: J.S., S.Z.; Funding acquisition: J.S., S.Z.

Funding

This work was supported by National Natural Science Foundation of China (NSFC) grants (31372258 and 31630070 to S.Z., and 31702063 to J.S.).

Data availability

RNA-seq data have been deposited in GEO under accession number GSE123150.

Supplementary information

Supplementary information available online at
http://dev.biologists.org/lookup/doi/10.1242/dev.170670.supplemental

References

Belles, X. (2017). MicroRNAs and the evolution of insect metamorphosis. *Annu. Rev. Entomol.* **62**, 111-125.
Belles, X. and Santos, C. G. (2014). The MEKRE93 (Methoprene tolerant-Krüppel homolog 1-E93) pathway in the regulation of insect metamorphosis, and the homology of the pupal stage. *Insect Biochem. Mol. Biol.* **52**, 60-68.
Belles, X., Cristino, A. S., Piulachs, M.-D., Rubio, M. and Tanaka, E. D. (2012). *Insect MicroRNAs: from Molecular Mechanisms to Biological Roles*. Elsevier Science B.V.
Bonci, D., Coppola, V., Musumeci, M., Addario, A., Giuffrida, R., Memeo, L., D'Urso, L., Pagliuca, A., Biffoni, M., Labbaye, C. et al. (2008). The miR-15a-miR-16-1 cluster controls prostate cancer by targeting multiple oncogenic activities. *Nat. Med.* **14**, 1271-1277.
Bryant, B., Macdonald, W. and Raikhel, A. S. (2010). microRNA miR-275 is indispensable for blood digestion and egg development in the mosquito *Aedes aegypti*. *Proc. Natl. Acad. Sci. USA* **107**, 22391-22398.
Caygill, E. E. and Johnston, L. A. (2008). Temporal regulation of metamorphic processes in *Drosophila* by the let-7 and miR-125 heterochronic microRNAs. *Curr. Biol.* **18**, 943-950.
Charles, J.-P., Iwema, T., Epa, V. C., Takaki, K., Rynes, J. and Jindra, M. (2011). Ligand-binding properties of a juvenile hormone receptor, Methoprene-tolerant. *Proc. Natl. Acad. Sci. USA* **108**, 21128-21133.
Chawla, G. and Sokol, N. S. (2012). Hormonal activation of let-7-C microRNAs via EcR is required for adult *Drosophila melanogaster* morphology and function. *Development* **139**, 1788-1797.
Chiu, J., March, P. E., Lee, R. and Tillett, D. (2004). Site-directed, Ligase-Independent Mutagenesis (SLIM): a single-tube methodology approaching 100% efficiency in 4 h. *Nucleic Acids Res.* **32**, e174.
Cui, Y., Sui, Y., Xu, J., Zhu, F. and Palli, S. R. (2014). Juvenile hormone regulates *Aedes aegypti* Krüppel homolog 1 through a conserved E box motif. *Insect Biochem. Mol. Biol.* **52**, 23-32.
Dhadialla, T. S., Cook, K. E. and Wyatt, G. R. (1987). Vitellogenin mRNA in locust fat body: coordinate induction of two genes by a juvenile hormone analog. *Dev. Biol.* **123**, 108-114.
Enright, A. J., John, B., Gaul, U., Tuschl, T., Sander, C. and Marks, D. S. (2003). MicroRNA targets in Drosophila. *Genome Biol.* **5**, R1.
Forman, J. J., Legesse-Miller, A. and Coller, H. A. (2008). A search for conserved sequences in coding regions reveals that the let-7 microRNA targets Dicer within its coding sequence. *Proc. Natl. Acad. Sci. USA* **105**, 14879-14884.
Ghildiyal, M. and Zamore, P. D. (2009). Small silencing RNAs: an expanding universe. *Nat. Rev. Genet.* **10**, 94-108.
Gujar, H. and Palli, S. R. (2016). Juvenile hormone regulation of female reproduction in the common bed bug, *Cimex lectularius*. *Sci. Rep.* **6**, 35546.
Guo, W., Wu, Z., Song, J., Jiang, F., Wang, Z., Deng, S., Walker, V. K. and Zhou, S. (2014). Juvenile hormone-receptor complex acts on mcm4 and mcm7 to promote polyploidy and vitellogenesis in the migratory locust. *PLoS Genet.* **10**, e1004702.
Hashimoto, Y., Akiyama, Y. and Yuasa, Y. (2013). Multiple-to-multiple relationships between microRNAs and target genes in gastric cancer. *PLoS ONE* **8**, e62589.
Jiang, J., Ge, X., Li, Z., Wang, Y., Song, Q., Stanley, D. W., Tan, A. and Huang, Y. (2013). MicroRNA-281 regulates the expression of ecdysone receptor (EcR) isoform B in the silkworm, *Bombyx mori*. *Insect Biochem. Mol. Biol.* **43**, 692-700.
Jindra, M., Palli, S. R. and Riddiford, L. M. (2013). The juvenile hormone signaling pathway in insect development. *Annu. Rev. Entomol.* **58**, 181-204.
Jindra, M., Bellés, X. and Shinoda, T. (2015a). Molecular basis of juvenile hormone signaling. *Curr. Opin. Insect Sci.* **11**, 39-46.
Jindra, M., Uhlirova, M., Charles, J.-P., Smykal, V. and Hill, R. J. (2015b). Genetic evidence for function of the bHLH-PAS protein Gce/Met as a juvenile hormone receptor. *PLoS Genet.* **11**, e1005394.
Kayukawa, T., Minakuchi, C., Namiki, T., Togawa, T., Yoshiyama, M., Kamimura, M., Mita, K., Imanishi, S., Kiuchi, M., Ishikawa, Y. et al. (2012). Transcriptional regulation of juvenile hormone-mediated induction of Kruppel homolog 1, a

repressor of insect metamorphosis. *Proc. Natl. Acad. Sci. USA* **109**, 11729-11734.
Kayukawa, T., Nagamine, K., Ito, Y., Nishita, Y., Ishikawa, Y. and Shinoda, T. (2016). Krüppel homolog 1 inhibits insect metamorphosis via direct transcriptional repression of broad-complex, a pupal specifier gene. *J. Biol. Chem.* **291**, 1751-1762.
Kayukawa, T., Jouraku, A., Ito, Y. and Shinoda, T. (2017). Molecular mechanism underlying juvenile hormone-mediated repression of precocious larval-adult metamorphosis. *Proc. Natl. Acad. Sci. USA* **114**, 1057-1062.
Kim, Y.-K., Yeo, J., Kim, B., Ha, M. and Kim, V. N. (2012). Short structured RNAs with low GC content are selectively lost during extraction from a small number of cells. *Mol. Cell* **46**, 893-895.
Konopova, B., Smykal, V. and Jindra, M. (2011). Common and distinct roles of juvenile hormone signaling genes in metamorphosis of holometabolous and hemimetabolous insects. *PLoS ONE* **6**, e28728.
Kozomara, A. and Griffiths-Jones, S. (2014). miRBase: annotating high confidence microRNAs using deep sequencing data. *Nucleic Acids Res.* **42**, D68-D73.
Lei, Z., Lv, Y., Wang, W., Guo, Q., Zou, F., Hu, S., Fang, F., Tian, M., Liu, B., Liu, X. et al. (2015). MiR-278-3p regulates pyrethroid resistance in *Culex pipiens pallens*. *Parasitol. Res.* **114**, 699-706.
Li, M., Mead, E. A. and Zhu, J. (2011). Heterodimer of two bHLH-PAS proteins mediates juvenile hormone-induced gene expression. *Proc. Natl. Acad. Sci. USA* **108**, 638-643.
Li, M., Liu, P., Wiley, J. D., Ojani, R., Bevan, D. R., Li, J. and Zhu, J. (2014). A steroid receptor coactivator acts as the DNA-binding partner of the methoprene-tolerant protein in regulating juvenile hormone response genes. *Mol. Cell. Endocrinol.* **394**, 47-58.
Ling, L., Ge, X., Li, Z., Zeng, B., Xu, J., Aslam, A. F. M., Song, Q., Shang, P., Huang, Y. and Tan, A. (2014). MicroRNA Let-7 regulates molting and metamorphosis in the silkworm, *Bombyx mori*. *Insect Biochem. Mol. Biol.* **53**, 13-21.
Liu, S., Li, K., Gao, Y., Liu, X., Chen, W., Ge, W., Feng, Q., Palli, S. R. and Li, S. (2018). Antagonistic actions of juvenile hormone and 20-hydroxyecdysone within the ring gland determine developmental transitions in *Drosophila*. *Proc. Natl. Acad. Sci. USA* **115**, 139-144.
Lozano, J. and Belles, X. (2011). Conserved repressive function of Krüppel homolog 1 on insect metamorphosis in hemimetabolous and holometabolous species. *Sci. Rep.* **1**, 163.
Lozano, J., Kayukawa, T., Shinoda, T. and Belles, X. (2014). A role for Taiman in insect metamorphosis. *PLoS Genet.* **10**, e1004769.
Lozano, J., Montanez, R. and Belles, X. (2015). MiR-2 family regulates insect metamorphosis by controlling the juvenile hormone signaling pathway. *Proc. Natl. Acad. Sci. USA* **112**, 3740-3745.
Lucas, K. and Raikhel, A. S. (2013). Insect microRNAs: biogenesis, expression profiling and biological functions. *Insect Biochem. Mol. Biol.* **43**, 24-38.
Lucas, K. J., Zhao, B., Roy, S., Gervaise, A. L. and Raikhel, A. S. (2015). Mosquito-specific microRNA-1890 targets the juvenile hormone-regulated serine protease JHA15 in the female mosquito gut. *RNA Biol.* **12**, 1383-1390.
Luo, M., Li, D., Wang, Z., Guo, W., Kang, L. and Zhou, S. (2017). Juvenile hormone differentially regulates two Grp78 genes encoding protein chaperones required for insect fat body cell homeostasis and vitellogenesis. *J. Biol. Chem.* **292**, 8823-8834.
Minakuchi, C., Zhou, X. and Riddiford, L. M. (2008). Krüppel homolog 1 (Kr-h1) mediates juvenile hormone action during metamorphosis of *Drosophila melanogaster*. *Mech. Dev.* **125**, 91-105.
Minakuchi, C., Namiki, T. and Shinoda, T. (2009). Krüppel homolog 1, an early juvenile hormone-response gene downstream of Methoprene-tolerant, mediates its anti-metamorphic action in the red flour beetle *Tribolium castaneum*. *Dev. Biol.* **325**, 341-350.
Ojani, R., Fu, X., Ahmed, T., Liu, P. and Zhu, J. (2018). Krüppel homologue 1 acts as a repressor and an activator in the transcriptional response to juvenile hormone in adult mosquitoes. *Insect Mol. Biol.* **27**, 268-278.
Raikhel, A. S., Brown, M. R. and Belles, X. (2005). Hormonal control of reproductive processes. In *Comprehensive Molecular Insect Science* (ed. L. I. Gilbert), pp. 433-491. Amsterdam: Elsevier.
Riddiford, L. M. (1994). Cellular and molecular actions of juvenile-hormone .1. General-considerations and premetamorphic actions. *Adv. Insect Physiol.* **24**, 213-274.
Rigoutsos, I. (2009). New tricks for animal microRNAS: targeting of amino acid coding regions at conserved and nonconserved sites. *Cancer Res.* **69**, 3245-3248.
Roy, S., Saha, T. T., Zou, Z. and Raikhel, A. S. (2018). Regulatory pathways controlling female insect reproduction. *Annu. Rev. Entomol.* **63**, 489-511.
Rubio, M. and Belles, X. (2013). Subtle roles of microRNAs let-7, miR-100 and miR-125 on wing morphogenesis in hemimetabolan metamorphosis. *J. Insect Physiol.* **59**, 1089-1094.
Rubio, M., de Horna, A. and Belles, X. (2012). MicroRNAs in metamorphic and non-metamorphic transitions in hemimetabolan insect metamorphosis. *BMC Genomics* **13**, 386.
Shin, S. W., Zou, Z., Saha, T. T. and Raikhel, A. S. (2012). bHLH-PAS heterodimer of methoprene-tolerant and Cycle mediates circadian expression of juvenile hormone-induced mosquito genes. *Proc. Natl. Acad. Sci. USA* **109**, 16576-16581.
Smykal, V., Daimon, T., Kayukawa, T., Takaki, K., Shinoda, T. and Jindra, M. (2014). Importance of juvenile hormone signaling arises with competence of insect larvae to metamorphose. *Dev. Biol.* **390**, 221-230.
Song, J., Wu, Z., Wang, Z., Deng, S. and Zhou, S. (2014). Krüppel-homolog 1 mediates juvenile hormone action to promote vitellogenesis and oocyte maturation in the migratory locust. *Insect Biochem. Mol. Biol.* **52**, 94-101.
Sun, Y., Li, Q., Gui, H., Xu, D.-P., Yang, Y.-L., Su, D.-F. and Liu, X. (2013). MicroRNA-124 mediates the cholinergic anti-inflammatory action through inhibiting the production of pro-inflammatory cytokines. *Cell Res.* **23**, 1270-1283.
Teleman, A. A., Maitra, S. and Cohen, S. M. (2006). *Drosophila* lacking microRNA miR-278 are defective in energy homeostasis. *Genes Dev.* **20**, 417-422.
Thadani, R. and Tammi, M. T. (2006). MicroTar: predicting microRNA targets from RNA duplexes. *BMC Bioinformatics* **7** Suppl. 5, S20.
Ureña, E., Chafino, S., Manjón, C., Franch-Marro, X. and Martín, D. (2016). The occurrence of the holometabolous pupal stage requires the interaction between E93, Krüppel-homolog 1 and broad-complex. *PLoS Genet.* **12**, e1006020.
Varghese, J. and Cohen, S. M. (2007). microRNA miR-14 acts to modulate a positive autoregulatory loop controlling steroid hormone signaling in *Drosophila*. *Genes Dev.* **21**, 2277-2282.
Wang, X., Fang, X., Yang, P., Jiang, X., Jiang, F., Zhao, D., Li, B., Cui, F., Wei, J., Ma, C. et al. (2014). The locust genome provides insight into swarm formation and long-distance flight. *Nat. Commun.* **5**, 2957.
Wang, Y., Jiang, F., Wang, H., Song, T., Wei, Y., Yang, M., Zhang, J. and Kang, L. (2015). Evidence for the expression of abundant microRNAs in the locust genome. *Sci. Rep.* **5**, 13608.
Wu, P., Qin, G., Qian, H., Chen, T. and Guo, X. (2016). Roles of miR-278-3p in IBP2 regulation and *Bombyx mori* cytoplasmic polyhedrosis virus replication. *Gene* **575**, 264-269.
Wu, Y., Li, X., Jia, J., Zhang, Y., Li, J., Zhu, Z., Wang, H., Tang, J. and Hu, J. (2018a). Transmembrane E3 ligase RNF183 mediates ER stress-induced apoptosis by degrading Bcl-xL. *Proc. Natl. Acad. Sci. USA* **115**, E2762-E2771.
Wu, Z., Guo, W., Yang, L., He, Q. and Zhou, S. (2018b). Juvenile hormone promotes locust fat body cell polyploidization and vitellogenesis by activating the transcription of Cdk6 and E2f1. *Insect Biochem. Mol. Biol.* **102**, 1-10.
Wyatt, G. R. and Davey, K. G. (1996). Cellular and molecular actions of juvenile hormone. II. Roles of juvenile hormone in adult insects. *Adv. Insect Physiol.* **26**, 1-155.
Yang, M., Wei, Y., Jiang, F., Wang, Y., Guo, X., He, J. and Kang, L. (2014). MicroRNA-133 inhibits behavioral aggregation by controlling dopamine synthesis in locusts. *PLoS Genet.* **10**, e1004206.
Zhang, T., Song, W., Li, Z., Qian, W., Wei, L., Yang, Y., Wang, W., Zhou, X., Meng, M., Peng, J. et al. (2018). Krüppel homolog 1 represses insect ecdysone biosynthesis by directly inhibiting the transcription of steroidogenic enzymes. *Proc. Natl. Acad. Sci. USA* **115**, 3960-3965.
Zhou, S., Zhang, J., Hirai, M., Chinzei, Y., Kayser, H., Wyatt, G. R. and Walker, V. K. (2002). A locust DNA-binding protein involved in gene regulation by juvenile hormone. *Mol. Cell. Endocrinol.* **190**, 177-185.
Zou, Z., Saha, T. T., Roy, S., Shin, S. W., Backman, T. W. H., Girke, T., White, K. P. and Raikhel, A. S. (2013). Juvenile hormone and its receptor, methoprene-tolerant, control the dynamics of mosquito gene expression. *Proc. Natl. Acad. Sci. USA* **110**, E2173-E2181.

Supplementary information

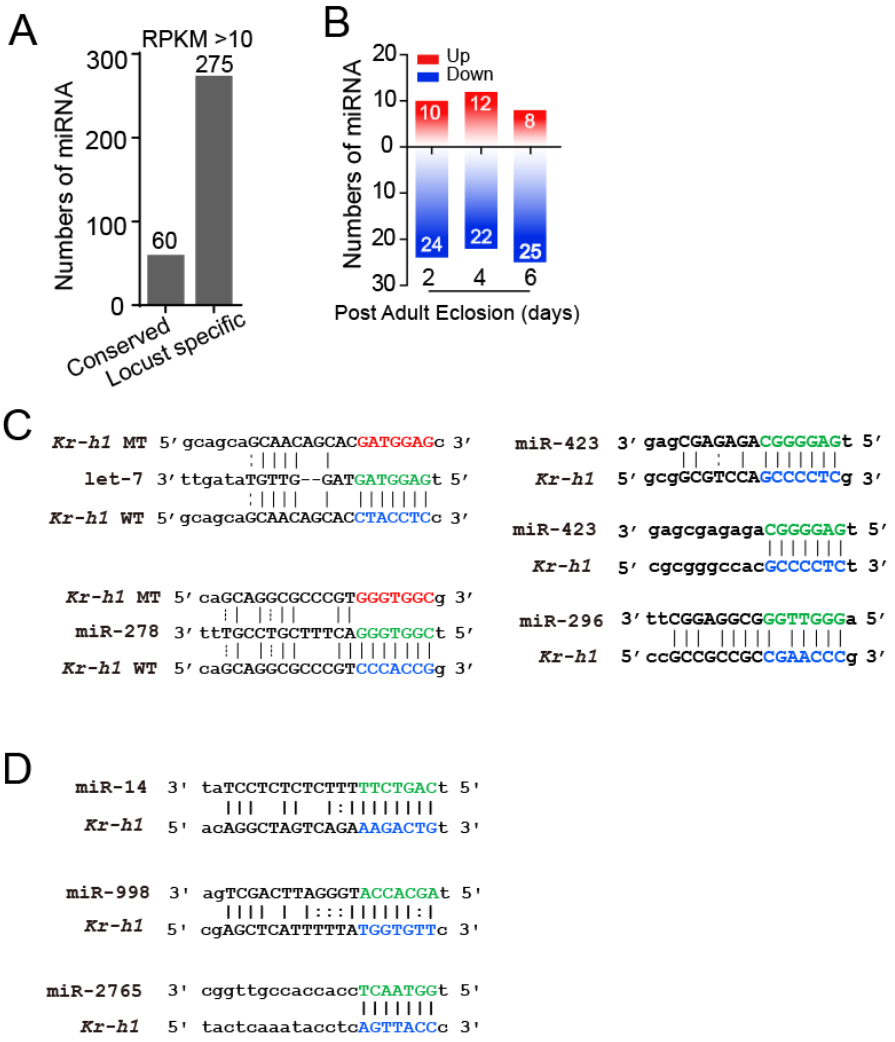

Fig. S1. **miRNA identification and binding site prediction for *Kr-h1*.** (A) Numbers of conserved miRNA and locust specific miRNA with RPKM values > 10. (B) The number of upregulated and downregulated miRNAs in the fat body of adult females at 2, 4 and 6 days post adult eclosion compared to that on the day of adult eclosion. (C, D) Sequence alignment of miRNAs with their predicted binding sites in the CDS (C) and 3′UTR (D) of *Kr-h1*. The binding sites (blue) in *Kr-h1* complementary to the seed region (green) of let-7 and miR-278 were site-mutated to their complementary bases (red) in the luciferase reporter assays.

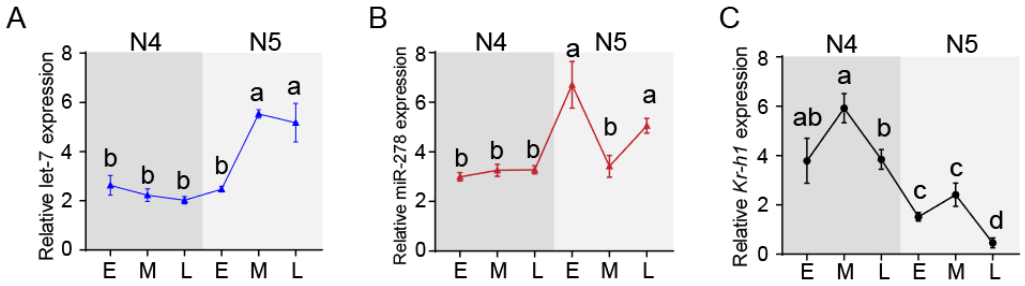

Fig. S2. The temporal expression patterns of let-7, miR-278 and *Kr-h1* in late-instar locust nymphs. qRT-PCR showing the relative levels of let-7 (A), miR-278 (B) and *Kr-h1* (C) expression in the whole body of penultimate 4th (N4) and final 5th (N5) instar nymphs. E, M, and L indicate the early (day 1), middle (day 2 for N4, and day 3 for N5), and late (day 4 for N4, and day 5 for N5) stages, respectively. The duration of 4th and 5th instar nymphs was about 4 days and 5 days, respectively under our reading conditions. In each panel, the means labeled with different letters indicate significant difference at $P < 0.05$. n = 8.

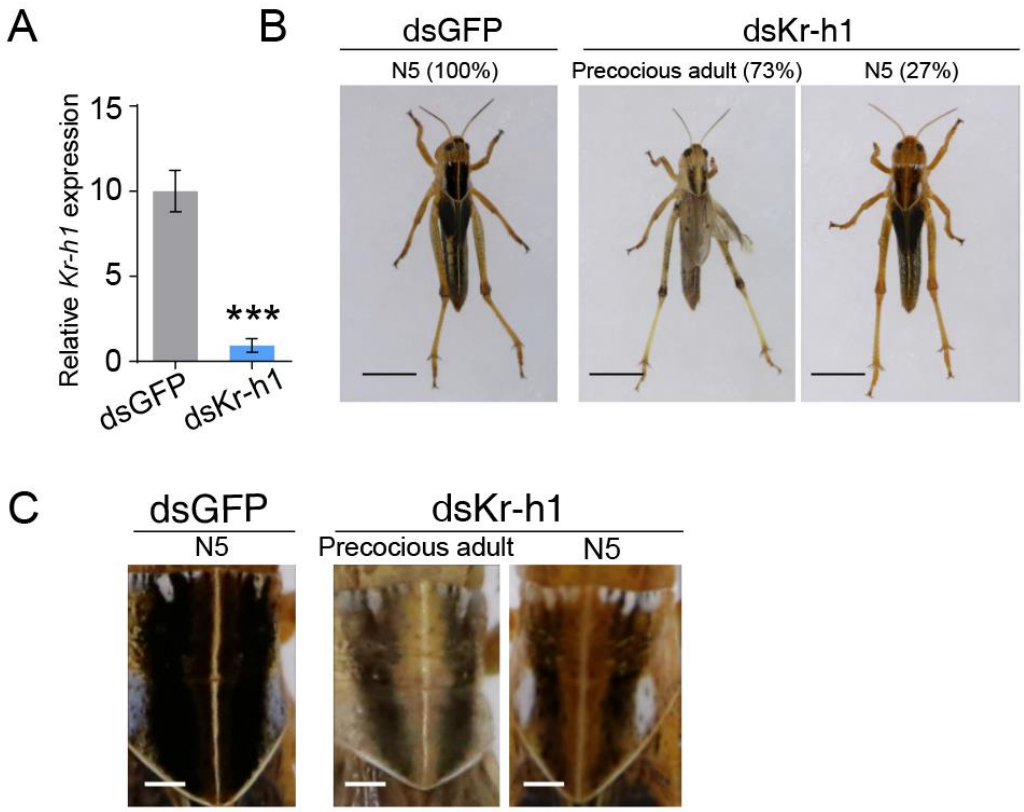

Fig. S3. Effect of *Kr-h1* knockdown on locust metamorphosis. (A) RNAi-mediated knockdown efficiency of *Kr-h1* in the whole body of final 5th instar nymphs previously subjected to dsKr-h1 treatment at the penultimate 4th nymphal instar. ***, $P < 0.001$ compared to the dsGFP control. n = 7-8. (B) Representative phenotypes and percentage of precocious metamorphosis at the final instar nymphs (N5) previously subjected to dsKr-h1 treatment at the penultimate 4th nymph instar (3 replicates with 7-8 locusts in each treatment). Scale bar, 1 cm. (C) Enlarged images of the pronotum shown in (B). Scale bar, 0.1 cm.

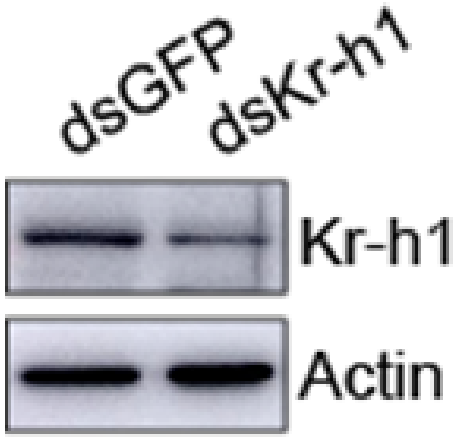

Fig. S4. Specificity of the antiserum. The antiserum specificity was verified by western blot using protein extracted from fat body of locusts treated with dsKr-h1 versus dsGFP.

Table S1. Primers used in qRT-PCR, mutation and RNAi.

Primer Name	Sequence (5' to 3')
qRT-PCR	
qKr-h1-F	ACTTCGTCTTCTGGAATGA
qKr-h1-R	GGCAATCGGTATTACACTTAG
qlet-7-F	GCTGAGGTAGTAGGTTGTATAGTT
qmiR-278-F	GGTGGGACTTTCGTCCGTTT
qU6	ACACTCCAGCTGGGTCAAAATCGTGAAGCG
qVgA-F	CCCACAAGAAGCACAGAACG
qVgA-R	TTGGTCGCCATCAACAGAAG
qActin-F	AATTACCATTGGTAACGAGCGATT
qActin-R	TGCTTCCATACCCAGGAATGA
site mutation	
mut-let-7-F	CCTCTGCTTGATGATGGAGTACTCGCAGCAGGCGCCCGTCCCAC
mut-let-7-R	CGAGTACTCCATCATCAAGCAGAGGTCGCGACCGCCCCCGGGCGT
mut-miR-278-F	GCGCCCGTTGATGACGCGCACGCGGGCCACGCCCCTCTCTCC
mut-miR-278-R	CGTGCGCGTCATCAACGGGCGCCTGCTGCGAGTACAGGTAGT
dsRNA synthesis	
dsKr-h1-F	GTCAAGGAGAACCTGAGCGTGC
dsKr-h1-R	TGCTGCTGCTCCGAGTGGCT
dsGFP-F	CACAAGTTCAGCGTGTCCG
dsGFP-R	GTTCACCTTGATGCCGTTC